

1 **A FANNING SCHEME FOR THE PARALLEL TRANSPORT ALONG**
2 **GEODESICS ON RIEMANNIAN MANIFOLDS**

3 MAXIME LOUIS^{1,2}, BENJAMIN CHARLIER^{3,1,2}, PAUL JUSSELIN^{4,1,2}, SUSOVAN
4 PAL^{1,2}, STANLEY DURRLEMAN^{1,2}

5 ¹INRIA PARIS, ARAMIS PROJECT-TEAM, 75013, PARIS, FRANCE

6 ²SORBONNE UNIVERSITÉS, UPMC UNIV PARIS 06, INSERM, CNRS, INSTITUT DU
7 CERVEAU ET DE LA MOELLE (ICM) - HÔPITAL PITIÉ-SALPÊTRIÈRE, BOULEVARD
8 DE L'HÔPITAL, F-75013, PARIS, FRANCE

9 ³INSTITUT MONTPELLIÉRAIN ALEXANDER GROTHENDIECK, CNRS, UNIV.
10 MONTPELLIER

11 ⁴CMLA, ENS CACHAN

12 **Abstract.** Parallel transport on Riemannian manifolds allows one to connect tangent spaces at
13 different points in an isometric way and is therefore of importance in many contexts, such as statistics
14 on manifolds. The existing methods to compute parallel transport require either the computation
15 of Riemannian logarithms, such as Schild's ladder, or the Christoffel symbols. The Logarithm is
16 rarely given in closed form, and therefore costly to compute whereas the Christoffel symbols are
17 in general hard and costly to compute. From an identity between parallel transport and Jacobi
18 fields, we propose a numerical scheme to approximate the parallel transport along a geodesic. We
19 find and prove an optimal convergence rate for the scheme, which is equivalent to Schild's ladder's.
20 We investigate potential variations of the scheme and give experimental results on the Euclidean
21 two-sphere and on the manifold of symmetric positive definite matrices.

22 **Key words.** Parallel Transport, Riemannian manifold, Numerical scheme, Jacobi field

23 **1. Introduction.** Riemannian geometry has been long contained within the field
24 of pure mathematics and theoretical physics. Nevertheless, there is an emerging trend
25 to use the tools of Riemannian geometry in statistical learning to define models for
26 structured data. Such data may be defined by invariance properties, and therefore
27 seen as points in quotient spaces as for shapes, orthogonal frames, or linear subspaces.
28 They may be defined also by smooth inequalities, and therefore as points in open
29 subsets of linear spaces, as for symmetric positive definite matrices, diffeomorphisms
30 or bounded measurements. Such data may be considered therefore as points in a
31 Riemannian manifolds, and analysed by specific statistical approaches [14, 3, 10, 4].
32 At the core of these approaches lies parallel transport, an isometry between tangent
33 spaces which allows the comparison of probability density functions, coordinates or
34 vectors that are defined in the tangent space at different points on the manifold. The
35 inference of such statistical models in practical situations requires efficient numerical
36 schemes to compute parallel transport on manifolds.

37 The parallel transport of a given tangent vector is defined as the solution of
38 an ordinary differential equation ([8] page 52), written in terms of the Christoffel
39 symbols. The computation of the Christoffel symbols requires access to the metric
40 coefficients and their derivatives, making the equation integration using standard nu-
41 merical schemes very costly in situations where no closed-form formulas are available
42 for the metric coefficients or their derivatives.

43 An alternative is to use Schild's ladder [2], or its faster version in the case of
44 geodesics, the pole ladder [6]. These schemes essentially require the computation of
45 Riemannian exponentials and logarithms at each step. Usually, the computation of
46 the exponential may be done by integrating Hamiltonian equations, and does not
47 raise specific difficulties. By contrast, the computation of the logarithm must often
48 be done by solving an inverse problem with the use of an optimization scheme such
49 as a gradient descent. Such optimization schemes are approximate and sensitive to

50 the initial conditions and to hyper-parameters, which leads to additional numerical
 51 errors –most of the time uncontrolled– as well as an increased computational cost. When
 52 closed formulas exist for the Riemannian logarithm, or in the case of Lie groups, where
 53 the Logarithm can be approximated efficiently using the Baker-Campbell-Hausdorff
 54 formula (see [5]), Schild’s ladder is an efficient alternative. When this is not the case,
 55 it becomes hardly tractable. [A more detailed analysis of the convergence of Schild’s](#)
 56 [ladder method can be found in \[9\]](#)

57 Another alternative is to use an equation showing that parallel transport along
 58 geodesics may be locally approximated by a well-chosen Jacobi field, up to the second
 59 order error. This idea has been suggested in [12] with further credits to [1], but
 60 without either a formal definition nor a proof of its convergence. It relies solely on
 61 the computations of Riemannian exponentials.

62 In this paper, we propose a numerical scheme built on this idea, which tries to limit
 63 as much as possible the number of operations required to reach a given accuracy. [We](#)
 64 [will show how to use only the inverse of the metric and its derivatives when performing](#)
 65 [the different steps of the scheme. This different set of requirements makes the scheme](#)
 66 [attractive in a different set of situations than the integration of the ODE or the Schild’s](#)
 67 [ladder.](#) We will prove that this scheme converges at linear speed with the time-
 68 step, and that this speed may not be improved without further assumptions on the
 69 manifold. Furthermore, we propose an implementation which allows the simultaneous
 70 computation of the geodesic and of the transport along this geodesic. Numerical
 71 experiments on the 2-sphere and on the manifold of 3-by-3 symmetric positive definite
 72 matrices will confirm that the convergence of the scheme is of the same order as
 73 Schild’s ladder in practice. Thus, they will show that this scheme offers a compelling
 74 alternative to compute parallel transport with a control over the numerical errors and
 75 the computational cost.

76 2. Rationale.

77 **2.1. Notations and assumptions.** In this paper, we assume that γ is a geo-
 78 desic defined for all time $t > 0$ on a smooth manifold \mathcal{M} of finite dimension $n \in \mathbb{N}$
 79 provided with a smooth Riemannian metric g . We denote the Riemannian exponential
 80 Exp and ∇ the covariant derivative. For $p \in \mathcal{M}$, $T_p\mathcal{M}$ denotes the tangent space of
 81 \mathcal{M} at p . For all $s, t \geq 0$ and for all $w \in T_{\gamma(s)}\mathcal{M}$, we denote $P_{s,t}(w) \in T_{\gamma(t)}\mathcal{M}$ the
 82 parallel transport of w from $\gamma(s)$ to $\gamma(t)$. It is the unique solution at time t of the
 83 differential equation $\nabla_{\dot{\gamma}(u)}P_{s,u}(w) = 0$ for $P_{s,s}(w) = w$. We also denote $J_{\gamma(t)}^w(h)$ the
 84 Jacobi field emerging from $\gamma(t)$ in the direction $w \in T_{\gamma(t)}\mathcal{M}$, that is

$$85 \quad J_{\gamma(t)}^w(h) = \left. \frac{\partial}{\partial \varepsilon} \right|_{\varepsilon=0} \text{Exp}_{\gamma(t)}(h(\dot{\gamma}(t) + \varepsilon w)) \in T_{\gamma(t+h)}\mathcal{M}$$

86 for $h \in \mathbb{R}$ small enough. It verifies the Jacobi equation (see for instance [8] page
 87 111-119)

$$88 \quad (1) \quad \nabla_{\dot{\gamma}}^2 J_{\gamma(t)}^w(h) + R(J_{\gamma(t)}^w(h), \dot{\gamma}(h))\dot{\gamma}(h) = 0$$

89 where R is the curvature tensor. We denote $\|\cdot\|_g$ the Riemannian norm on the tangent
 90 spaces defined from the metric g , and $g_p : T_p\mathcal{M} \times T_p\mathcal{M} \rightarrow \mathbb{R}$ the metric at any $p \in \mathcal{M}$.
 91 We use Einstein notations.

92 We fix Ω a compact subset of \mathcal{M} such that Ω contains a neighborhood of $\gamma([0, 1])$.
 93 [We also set \$w \in T_{\gamma\(0\)}\mathcal{M}\$ and \$w\(t\) = P_{0,t}\(w\)\$.](#) [We suppose that there exists a coordinate](#)
 94 [system on \$\Omega\$ and we denote \$\Phi : \Omega \rightarrow U\$ the corresponding diffeomorphism, where \$U\$](#)

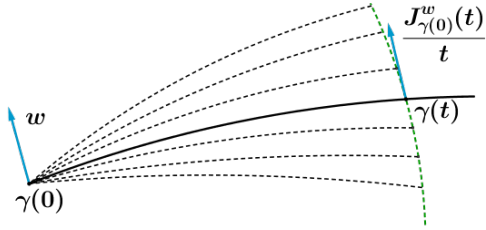


FIGURE 1. The solid line is the geodesic. The green dotted line is formed by the perturbed geodesics at time t . The blue arrows are the initial vector and its approximated parallel transport at time t .

95 is a subset of \mathbb{R}^n . This system of coordinates allows us to define a basis of the tangent
 96 space of \mathcal{M} at any point of Ω , we denote $\frac{\partial}{\partial x^i} \Big|_p$ the i -th element of the corresponding
 97 basis of $T_p\mathcal{M}$ for any $p \in \mathcal{M}$. Note finally that, since the injectivity radius is a smooth
 98 function of the position on the manifold (see [8]) and that it is everywhere positive
 99 on Ω , there exists $\eta > 0$ such that for all p in Ω , the injectivity radius at p is larger
 100 than η .

101 The problem in this paper is to provide a way to compute an approximation of
 102 $P_{0,1}(w)$.

103 We suppose throughout the paper the existence of a single coordinate chart defined on Ω . In this setting, we propose a numerical scheme which gives an error varying
 104 linearly with the size of the integration step. Once this result is established, since in
 105 any case $\gamma([0, 1])$ can be covered by finitely many charts, it is possible to apply the
 106 proposed method to parallel transport on each chart successively. The errors during
 107 this computation of the parallel transport transport would add, but the convergence
 108 result remains valid.
 109
 110

111 **2.2. The key identity.** The numerical scheme that we propose arises from the
 112 following identity, which is mentioned in [12]. Figure 1 illustrates the principle.

113 PROPOSITION 2.1. For all $t > 0$, and $w \in T_{\gamma(0)}\mathcal{M}$ we have

114 (2)
$$P_{0,t}(w) = \frac{J_{\gamma(0)}^w(t)}{t} + O(t^2).$$

115 *Proof.* Let $X(t) = P_{0,t}(w)$ be the vector field following the parallel transport
 116 equation: $\dot{X}^i + \Gamma_{kl}^i X^l \dot{\gamma}^k = 0$ with $X(0) = w$, where $(\Gamma_{kl}^i)_{i,j,k \in \{1, \dots, n\}}$ are the Christoffel
 117 symbols associated with the Levi-Civita connection for the metric g . In normal
 118 coordinates centered at $\gamma(0)$, the Christoffel symbols vanish at $\gamma(0)$ and the equation
 119 gives: $\dot{X}^i(0) = 0$. A Taylor expansion of $X(t)$ near $t = 0$ in this local chart then reads

120 (3)
$$X^i(t) = w^i + O(t^2).$$

121 By definition, the i -th normal coordinate of $\text{Exp}_{\gamma(0)}(t(v_0 + \varepsilon w))$ is $t(v_0^i + \varepsilon w^i)$. There-
 122 fore, the i -th coordinate of $J_{\gamma(0)}^w(t) = \frac{\partial}{\partial \varepsilon} \Big|_{\varepsilon=0} \text{Exp}_{\gamma(0)}(t(\dot{\gamma}(0) + \varepsilon w))$ is tw^i . Plugging
 123 this into (3) yields the desired result. \square

124 This control on the approximation of the transport by a Jacobi field suggests
 125 to divide $[0, 1]$ into N intervals $[\frac{k}{N}, \frac{k+1}{N}]$ of length $h = \frac{1}{N}$ for $k = 0, \dots, N - 1$ and

126 to approximate the parallel transport of a vector $w \in T_{\gamma(0)}$ from $\gamma(0)$ to $\gamma(1)$ by a
 127 sequence of vectors $w_k \in T_{\gamma(\frac{k}{N})}\mathcal{M}$ defined as

$$128 \quad (4) \quad \begin{cases} w_0 = w \\ w_{k+1} = NJ_{\gamma(\frac{k}{N})}^{w_k} \left(\frac{1}{N} \right). \end{cases}$$

129 With the control given in the Proposition 2.1, we can expect to get an error of order
 130 $O(\frac{1}{N^2})$ at each step and hence a speed of convergence in $O(\frac{1}{N})$ overall. There are
 131 manifolds for which the approximation of the parallel transport by a Jacobi field is
 132 exact e.g. Euclidean space, but in the general case, one cannot expect to get a better
 133 convergence rate. Indeed, we show in the next Section that this scheme for the sphere
 134 \mathbb{S}^2 has a speed of convergence exactly proportional to $\frac{1}{N}$.

135 **2.3. Convergence rate on \mathbb{S}^2 .** In this Section, we assume that one knows the
 136 geodesic path $\gamma(t)$ and how to compute any Jacobi fields without numerical errors,
 137 and show that the approximation due to Equation (2) alone raises a numerical error
 138 of order $O(\frac{1}{N})$.

139 Let $p \in \mathbb{S}^2$ and $v \in T_p\mathbb{S}^2$. (p and v are seen as vectors in \mathbb{R}^3). The geodesics are
 140 the great circles, which may be written as

$$141 \quad \gamma(t) = \text{Exp}_p(tv) = \cos(t|v|)p + \sin(t|v|)\frac{v}{|v|},$$

142 where $|\cdot|$ is the euclidean norm on \mathbb{R}^3 . Using spherical coordinates (θ, ϕ) on the sphere,
 143 chosen so that the whole geodesic is in the coordinate chart, we get coordinates on
 144 the tangent space at any point $\gamma(t)$. In this spherical system of coordinates, it is
 145 straightforward to see that the parallel transport of $w = p \times v$ along $\gamma(t)$ has constant
 146 coordinates, where \times denote the usual cross-product on \mathbb{R}^3 .

147 We assume now that $|v| = 1$. Since $w = p \times v$ is orthogonal to v , we have
 148 $\frac{\partial}{\partial \varepsilon} \Big|_{\varepsilon=0} |v + \varepsilon w| = 0$. Therefore,

$$149 \quad \begin{aligned} J_p^w(t) &= \frac{\partial}{\partial \varepsilon} \Big|_{\varepsilon=0} \left(\cos(t|v + \varepsilon w|)p + \sin(t|v + \varepsilon w|)\frac{v + \varepsilon w}{|v + \varepsilon w|} \right) \\ &= \sin(t)w \end{aligned}$$

150 which does not depend on p . We have $J_{\gamma(t)}^w(t) = \sin(t)w$. Consequently, the se-
 151 quence of vectors w_k built by the iterative process described in equation (4) verifies
 152 $w_{k+1} = Nw_k \sin(\frac{1}{N})$ for $k = 0, \dots, N-1$, and $w_N = w_0 N \sin(\frac{1}{N})^N$. Now in the
 153 spherical coordinates, $P_{0,1}(w_0) = w_0$, so that the numerical error, measured in these
 154 coordinates, is proportional to $w_0 \left(1 - \left(\frac{\sin(1/N)}{1/N} \right)^N \right)$. We have

$$155 \quad \left(\frac{\sin(1/N)}{1/N} \right)^N = \exp \left(N \log \left(1 - \frac{1}{6N^2} + o(1/N^2) \right) \right) = 1 - \frac{1}{6N} + o\left(\frac{1}{N}\right)$$

156 yielding

$$157 \quad \frac{|w_N - w_0|}{|w_0|} \propto \frac{1}{6N} + o\left(\frac{1}{N}\right).$$

158 It shows a case where the bound $\frac{1}{N}$ is reached.

159 **3. The numerical scheme.**

160 **3.1. The algorithm.** In general, there are no closed forms expressions for the
 161 geodesics and the Jacobi fields. Hence, in most practical cases, these quantities also
 162 need to be computed using numerical methods.

163 *Computing geodesics.* In order to avoid the computation of the Christoffel sym-
 164 bols, we propose to integrate the first-order Hamiltonian equations to compute geo-
 165 desics. Let $x(t) = (x_1(t), \dots, x_d(t))^T$ be the coordinates of $\gamma(t)$ in a given local chart,
 166 and $\alpha(t) = (\alpha_1(t), \dots, \alpha_d(t))^T$ be the coordinates of the momentum $g_{\gamma(t)}(\dot{\gamma}(t), \cdot) \in$
 167 $T_{\gamma(t)}^* \mathcal{M}$ in the same local chart. We have then (see [13])

$$168 \quad (5) \quad \begin{cases} \dot{x}(t) = K(x(t))\alpha(t) \\ \dot{\alpha}(t) = -\frac{1}{2}\nabla_x (\alpha(t)^T K(x(t))\alpha(t)) \end{cases},$$

169 where $K(x(t))$, a d -by- d matrix, is the inverse of the metric g expressed in the local
 170 chart. Note that using (5) to integrate the geodesic equation will require us to convert
 171 initial tangent vectors into initial momenta, as seen in the algorithm description below.

172 *Computing $J_{\gamma(t)}^w(h)$.* The Jacobi field may be approximated with a numerical
 173 differentiation from the computation of a perturbed geodesic with initial position $\gamma(t)$
 174 and initial velocity $\dot{\gamma}(t) + \varepsilon w$ where ε is a small parameter

$$175 \quad (6) \quad J_{\gamma(t)}^w(h) \simeq \frac{\text{Exp}_{\gamma(t)}(h(\dot{\gamma}(t) + \varepsilon w)) - \text{Exp}_{\gamma(t)}(h\dot{\gamma}(t))}{\varepsilon},$$

176 where the Riemannian exponential may be computed by integration of the Hamilto-
 177 nian equations (5) over the time interval $[t, t+h]$ starting at point $\gamma(t)$, as shown on
 178 Figure 2. We will also see that a choice for ε ensuring a $O(\frac{1}{N})$ order of convergence
 179 is $\varepsilon = \frac{1}{N}$.

180 *The algorithm.* Let $N \in \mathbb{N}$. We divide $[0, 1]$ into N intervals $[t_k, t_{k+1}]$ with $t_k = \frac{k}{N}$
 181 and denote $h = \frac{1}{N}$ the size of the integration step. We initialize $\gamma_0 = \gamma(0)$, $\dot{\gamma}_0 = \dot{\gamma}(0)$,
 182 $\tilde{w}_0 = w$ and solve $\tilde{\beta}_0 = K^{-1}(\gamma_0)\tilde{w}_0$ and $\tilde{\alpha}_0 = K^{-1}(\gamma_0)\dot{\gamma}_0$. We use “ $\hat{\cdot}$ ” for quantities
 183 computed in the scheme without any renormalization and “ $\tilde{\cdot}$ ” for quantities computed
 184 in the scheme which have been renormalized to enforce expected conservations during
 185 the parallel transport. We propose to compute, at step k :

- 187 (i) The new point $\tilde{\gamma}_{k+1}$ and momentum $\tilde{\alpha}_{k+1}$ of the main geodesic, by performing
 188 one step of length h of a second-order Runge-Kutta method on equation (5).
 189 (ii) The perturbed geodesic starting at $\tilde{\gamma}_k$ with initial momentum $\tilde{\alpha}_k + \varepsilon\tilde{\beta}_k$ at time
 190 h , that we denote $\tilde{\gamma}_{k+1}^\varepsilon$, by performing one step of length h of a second-order
 191 Runge-Kutta method on equation (5).
 192 (iii) The estimated parallel transport before renormalization

$$193 \quad (7) \quad \hat{w}_{k+1} = \frac{\tilde{\gamma}_{k+1}^\varepsilon - \tilde{\gamma}_{k+1}}{h\varepsilon}.$$

194 (iv) The corresponding momentum $\hat{\beta}_{k+1}$, by solving: $K(\tilde{\gamma}_{k+1})\hat{\beta}_{k+1} = \hat{w}_{k+1}$.

(v) The renormalized version of this momentum, and the corresponding vector

$$\begin{aligned} \tilde{\beta}_{k+1} &= a_k \hat{\beta}_{k+1} + b_k \tilde{\alpha}_{k+1} \\ \tilde{w}_{k+1} &= K(\tilde{\gamma}_{k+1})\tilde{\beta}_{k+1} \end{aligned}$$

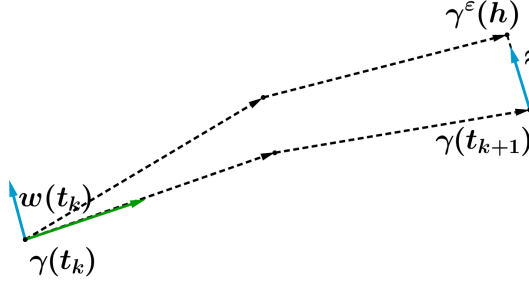


FIGURE 2. One step of the numerical scheme. The dotted arrows represent the steps of the Runge-Kutta integrations for the main geodesic γ and for the perturbed geodesic γ^ε . The blue arrows are the initial $w(t_k)$ and the obtained approximated transport using equation (6), with $h = t_{k+1} - t_k$.

195 where a_k and b_k are factors ensuring $\tilde{\beta}_{k+1}^\top K(\tilde{\gamma}(t))\tilde{\beta}_{k+1} = \beta_0^\top K(\gamma_0)\beta_0$ and
 196 $\tilde{\beta}_{k+1}^\top K(\tilde{\gamma}(t))\tilde{\alpha}_{k+1} = \beta_0^\top K(\gamma_0)\alpha_0$: quantities which should be conserved during
 197 the transport.

198 At the end of the scheme, \tilde{w}_N is the proposed approximation of $P_{0,1}(w)$. Figure 2
 199 illustrates the principle. A complete pseudo-code is given in appendix A. It is remark-
 200 able that we can substitute the computation of the Jacobi field with only four calls to
 201 the Hamiltonian equations (5) at each step, including the calls necessary to compute
 202 the main geodesic. Note however that the (iv) step of the algorithm requires to solve
 203 a linear system of size n . Solving the linear system can be done with a complexity less
 204 than cubic in the dimension (in $O(n^{2.374})$) using Coppersmith–Winograd algorithm).

205 **3.2. Possible variations.** There are a few possible variations of the presented
 206 algorithm.

- 207 1. The first variation is to use higher-order Runge-Kutta methods to integrate
 208 the geodesic equations at step (i) and (ii). We prove that a second-order
 209 integration of the geodesic equation is enough to guarantee convergence, and
 210 noticed experimentally the absence of convergence with a first order integra-
 211 tion of the geodesic equation.
- 212 2. The second variation is to replace step (ii) and step (iii) the following way. At
 213 the k -th iteration, compute two perturbed geodesics starting at $\tilde{\gamma}_k$ and with
 214 initial momentum $\tilde{\alpha}_k + \varepsilon\tilde{\beta}_k$ (resp. $\tilde{\alpha}_k - \varepsilon\tilde{\beta}_k$) at time h , that we denote $\tilde{\gamma}_{k+1}^{+\varepsilon}$
 215 (resp. $\tilde{\gamma}_{k+1}^{-\varepsilon}$), by performing one step of length h of a second-order Runge-
 216 Kutta method on equation (5). Then proceed to a second-order differentiation
 217 to approximate the Jacobi field, and set:

$$218 \quad (8) \quad \hat{w}_{k+1} = \frac{\tilde{\gamma}_{k+1}^{+\varepsilon} - \tilde{\gamma}_{k+1}^{-\varepsilon}}{2h\varepsilon}.$$

- 219
- 220 3. The final variation of the scheme consists in skipping step (v) and set $\tilde{w}_{k+1} =$
 221 \hat{w}_{k+1} and $\tilde{\beta}_{k+1} = \hat{\beta}_{k+1}$.

222 We will show that the proposed algorithm and these variations ensure convergence
 223 of the final estimate. Note that the best accuracy for a given computational cost is
 224 not necessarily obtained with the method in Section 3.1, but might be attained with
 225 one of the proposed variations, as a bit more computations at each step may be
 226 counter-balanced by a smaller constant in the convergence rate.

227 **3.3. The convergence Theorem.** We obtained the following convergence re-
 228 sult, guaranteeing a linear decrease of the error with the size of the step h .

229 **THEOREM 3.1.** *We suppose here the hypotheses stated in Section 2.1. Let $N \in \mathbb{N}$*
 230 *be the number of integration steps. Let $w \in T_{\gamma(0)}\mathcal{M}$ be the vector to be transported.*
 231 *We denote the error*

$$232 \quad \delta_k = \|P_{0,t_k}(w) - \tilde{w}_k\|_2$$

233 *where \tilde{w}_k is the approximate value of the parallel transport of w along γ at time t_k and*
 234 *where the 2-norm is taken in the coordinates of the chart Φ on Ω . We denote ε the*
 235 *parameter used in the step (ii) and $h = \frac{1}{N}$ the size of the step used of the Runge-Kutta*
 236 *approximate solution of the geodesic equation.*
 237 *If we take $\varepsilon = h$, then we have*

$$238 \quad \delta_N = O\left(\frac{1}{N}\right).$$

239 We will see in the proof and in the numerical experiments that choosing $\varepsilon = h$ is
 240 a recommended choice for the size of the step in the differentiation of the perturbed
 241 geodesics. Further decreasing ε has no visible effect on the accuracy of the estimation
 242 and choosing a larger ε lowers the quality of the approximation.

243 Note that our result controls the 2-norm of the error in the global system of
 244 coordinates, but not directly the metric norm in the tangent space at $\gamma(1)$. This is
 245 due to the fact that $\gamma(1)$ is not accessible, but only its approximation $\tilde{\gamma}_N$ computed
 246 by the Runge-Kutta integration of the Hamiltonian equation. However, Theorem
 247 3.1 implies that the couple $(\tilde{\gamma}_N, \tilde{w}_N)$ converges towards $(\gamma(1), P_{0,1}(w))$ using the ℓ^2
 248 distance on $\mathcal{M} \times T\mathcal{M}$ using a coordinate system in a neighborhood of $\gamma(1)$, which is
 249 equivalent to any distance on $\mathcal{M} \times T\mathcal{M}$ on this neighborhood and hence is the right
 250 notion of convergence.

251 We give the proof in the next Section. The technical lemmas used in the proof
 252 are all in the appendix: in Appendix B.1, we prove an intermediate result allowing
 253 uniform controls on norms of tensors, in Appendix B.3, we prove a stronger result
 254 than Proposition 2.1 with stronger hypotheses and in Appendix B.4, we prove a result
 255 allowing to control the accumulation of the error.

256 **4. Proof of the convergence Theorem 3.1.** We start by proving convergence
 257 without step (v) of the algorithm, i.e. without enforcing the conservations during
 258 the transport. Once the convergence of this variation is established, we prove the
 259 convergence with the step (v).

260 *Proof.* (Without step (v)) We will denote, as in the description of the algorithm
 261 in Section 3, $\gamma_k = \gamma(t_k)$, $\tilde{\gamma}_k = \tilde{\gamma}(t_k)$ its approximation in the algorithm. Let N be a
 262 number of discretization step and $k \in \{1, \dots, N\}$. We build an upper bound on the
 263 error δ_{k+1} from δ_k . We have

$$264 \quad \begin{aligned} \delta_{k+1} &= \|w_{k+1} - \tilde{w}_{k+1}\|_2 \\ &\leq \underbrace{\left\| w_{k+1} - \frac{J_{\gamma_k}^{w_k}(h)}{h} \right\|_2}_{(1)} + \underbrace{\left\| \frac{J_{\gamma_k}^{w_k}(h)}{h} - \frac{J_{\gamma_k}^{\tilde{w}_k}(h)}{h} \right\|_2}_{(2)} \\ &\quad + \underbrace{\left\| \frac{J_{\gamma_k}^{\tilde{w}_k}(h)}{h} - \frac{J_{\tilde{\gamma}_k}^{\tilde{w}_k}(h)}{h} \right\|_2}_{(3)} + \underbrace{\left\| \frac{J_{\tilde{\gamma}_k}^{\tilde{w}_k}(h)}{h} - \frac{\tilde{J}_{\tilde{\gamma}_k}^{\tilde{w}_k}(h)}{h} \right\|_2}_{(4)} \end{aligned}$$

265 where

- 266 • $\tilde{\gamma}_k$ is the approximation of the geodesic coordinates at step k .
- 267 • $w_k = w(t_k)$ is the exact parallel transport.
- 268 • \tilde{w}_k is its approximation at step k
- 269 • \tilde{J} is the approximation of the Jacobi field computed with finite difference:
- 270
$$\tilde{J}_{\tilde{\gamma}_k}^{\tilde{w}_k} = \frac{\tilde{\gamma}_{k+1}^\varepsilon - \tilde{\gamma}_{k+1}}{\varepsilon}.$$
- 271 • $J_{\tilde{\gamma}_k}^{\tilde{w}_k}(h)$ is the exact Jacobi field computed with the approximations \tilde{w} , $\tilde{\gamma}$ and
- 272 $\tilde{\gamma}$ *i.e.* the Jacobi field defined from the geodesic with initial position $\tilde{\gamma}_k$, initial
- 273 momentum $\tilde{\alpha}_k$, with a perturbation \tilde{w}_k .

274 We provide upper bounds for each of these terms. We start by assuming $\|w_k\|_2 \leq$
 275 $2\|w_0\|_2$, before showing it is verified for any $k \leq N$ when N is large enough. We
 276 could assume more generally $\|w_k\|_2 \leq C\|w_0\|_2$ for any $C > 1$. The idea is to get a
 277 uniform control on the errors at each step by assuming that $\|w_k\|_2$ does not grow too
 278 much, and show afterwards that the control we get is tight enough to ensure, when
 279 the number of integration steps is large, that we do have $\|w_k\|_2 \leq 2\|w_0\|_2$.

280 *Term (1).* This is the intrinsic error when using the Jacobi field. We show in
 281 Proposition B.3 that for h small enough

$$282 \quad \left\| P_{t_k, t_{k+1}}(w_k) - \frac{J_{\gamma_k}^{w_k}(h)}{h} \right\|_{g(\gamma(t_{k+1}))} \leq Ah^2 \|w_k\|_g = Ah^2 \|w_k\|_g.$$

283 Now, since g varies smoothly and by equivalence of the norms, there exists $A' > 0$
 284 such that

$$285 \quad (9) \quad \left\| P_{t_k, t_{k+1}}(w_k) - \frac{J_{\gamma^{(k)}}^{w_k}(h)}{h} \right\|_2 \leq A'h^2 \|w_k\|_2 \leq 2A'h^2 \|w_0\|_2$$

286 *Term (2).* Lemma B.4 show that for h small enough

$$287 \quad (10) \quad \left\| \frac{J_{\gamma(t_k)}^{w_k}(h)}{h} - \frac{J_{\gamma(t_k)}^{\tilde{w}_k}(h)}{h} \right\|_2 \leq (1 + Bh)\delta_k.$$

288 *Term (3).* This term measures the error linked to our approximate knowledge of
 289 the geodesic γ . It is proved in Appendix B.5 that there exists a constant $C > 0$ which
 290 does not depend on k or h such that :

$$291 \quad (11) \quad \left\| \frac{J_{\gamma_k}^{\tilde{w}_k}(h)}{h} - \frac{\tilde{J}_{\gamma_k}^{\tilde{w}_k}(h)}{h} \right\|_2 \leq Ch^2.$$

292 *Term (4).* This is the difference between the analytical computation of J and
 293 its approximation. It is proved in Appendix B.6 and B.7 that if we use a Runge-
 294 Kutta method of order 2 to compute the geodesic points γ_{k+1}^ε and γ_{k+1} and a first-
 295 order differentiation to compute the Jacobi field as described in the step (iii) of the
 296 algorithm, or if we use two perturbed geodesics γ_{k+1}^ε and $\gamma_{k+1}^{-\varepsilon}$ and a second-order
 297 differentiation method to compute the Jacobi field as described in equation (8), there
 298 exists $D \geq 0$ which does not depend on k such that:

$$299 \quad (12) \quad \left\| \frac{J_{\gamma(t_k)}^{\tilde{w}_k} - \tilde{J}_{\gamma(t_k)}^{\tilde{w}_k}}{h} \right\|_2 \leq D(h^2 + \varepsilon h)$$

300 Note that this majoration is valid as long as \tilde{w}_k is bounded by a constant which does
 301 not depend on k or N , which we have assumed so far.

302

303 Gathering equations (9), (10), (11) and (12), there exists a constant $F > 0$ such
 304 that for all k such that $\|w_i\|_2 \leq \|w_0\|_2$ for all $i \leq k$:

$$305 \quad (13) \quad \delta_{k+1} \leq (1 + Bh)\delta_k + F(h^2 + h\varepsilon).$$

306 Combining those inequalities for $k = 1, \dots, s$ where $s \in \{1, \dots, N\}$ is such that
 307 $\|w_k\|_2 \leq 2\|w_0\|_2$ for all $k \leq s$, we obtain a geometric series whose sum yields

$$308 \quad (14) \quad \delta_s \leq \frac{F(h^2 + h\varepsilon)}{Bh} (1 + Bh)^{s+1}.$$

309 We now show that for a large enough number of integration steps N , this implies that
 310 $\|w_k\|_2 \leq 2\|w_0\|_2$ for all $k \in \{1, \dots, N\}$. We proceed by contradiction, assuming that
 311 there exist arbitrary large $N \in \mathbb{N}$ for which there exists $u(N) \leq N$ – that we take
 312 minimal – such that $\|w_{u(N)}\|_2 > 2\|w_0\|_2$. For any such $N \in \mathbb{N}$, since $u(N)$ is minimal
 313 with that property, we can still use equation (14) with $s = u(N)$:

$$314 \quad (15) \quad \delta_{u(N)} \leq \frac{F(h^2 + h\varepsilon)}{Bh} (1 + Bh)^{u(N)+1}.$$

315 Now, $h = \frac{1}{N}$ so that

$$316 \quad (16) \quad \delta_{u(N)} \leq \frac{F(h + \varepsilon)}{B} (1 + Bh)^{u(N)+1} \leq \frac{F(h + \varepsilon)}{B} (1 + Bh)^{\frac{1}{h}+1}.$$

317 But we have, on the other hand:

$$318 \quad (17) \quad \|w_0\|_2 < \|\tilde{w}_{u(N)}\|_2 - \|w_0\|_2 \leq \|\tilde{w}_{u(N)} - w_0\|_2 \leq \frac{F(h + \varepsilon)}{B} (1 + Bh)^{\frac{1}{h}+1}$$

319 Taking $\varepsilon \leq h$, which we will keep as an assumption in the rest of the proof, the term
 320 on the right goes to zero as $h \rightarrow 0$ – i.e. as $N \rightarrow \infty$ – which is a contradiction.
 321 So for N large enough, we have $\|w_k\|_2 \leq 2\|w_0\|_2$ and equation (14) holds for all
 322 $k \in \{1, \dots, N\}$. With $s = N$, equation (14) reads:

$$323 \quad \delta_N \leq \frac{F(h^2 + h\varepsilon)}{Bh} (1 + Bh)^{N+1}.$$

324 We see that choosing $\varepsilon = \frac{1}{N}$ yields an optimal rate of convergence: choosing a larger
 325 value deteriorates the accuracy of the scheme while choosing a lower value still yields
 326 an error in $O(\frac{1}{N})$. Setting $\varepsilon = \frac{1}{N}$:

$$327 \quad \delta_N \leq \frac{2F}{BN} \left(1 + \frac{B}{N}\right)^{N+1} = \frac{2F}{BN} \left(\exp(B) + o\left(\frac{1}{N}\right)\right).$$

328 Eventually, there exists $G > 0$ such that, for $N \in \mathbb{N}$ large enough

$$329 \quad \delta_N \leq \frac{G}{N}. \quad \square$$

330 We now prove Theorem 3.1 when step (v) is used.

331 *Proof.* (With step (v)) The idea in this proof is to use equation (13) and the fact
 332 that when \hat{w}_{j+1} is close enough to w_{j+1} , step (v) necessarily improves the approxima-
 333 tion. As in the algorithm description, we denote \hat{w}_k the estimate before step (v) and

334 \tilde{w}_k the renormalized estimate. We now denote $\delta_k = \|w_k - \tilde{w}_k\|_2$. We use equation
335 (13), which now reads

$$336 \quad (18) \quad \|w_{k+1} - \hat{w}_{k+1}\|_2 \leq (1 + Bh)\delta_k + F(h^2 + h\varepsilon).$$

337 For $t \in [0, 1]$, let's denote $P_t : T_{\gamma(t)}\mathcal{M} \rightarrow T_{\gamma(t)}\mathcal{M}$ the operator defined at step (v): for
338 $z \in T_{\gamma(t)}\mathcal{M}$, $P(t, z)$ is the renormalized version of z to respect the conservations during
339 parallel transport. Step (v) now reads $P(t_k, \hat{w}_k) = \tilde{w}_k$. For any $t \in [0, 1]$, we have
340 $P(t, w(t)) = w(t)$ so that $z \rightarrow \|P(t, z) - w(t)\|_2^2$ is smooth and has a local minimum
341 at $w(t)$, so that its differential is zero at $w(t)$. Since P_t continuously varies with t ,
342 there exists $r > 0$ such that, for all $t \in [0, 1]$, for all $z \in T_{\gamma(t)}\mathcal{M}$ with $\|w(t) - z\|_2 \leq r$:

$$343 \quad (19) \quad \|w(t) - P(t, z)\|_2 \leq \|w(t) - z\|_2$$

344 Now for N large enough and $k \in \{1, \dots, N\}$, assuming δ_k small enough will ensure
345 $\|w_k - \hat{w}_k\| \leq r$ as shown in equation (18) so that:

$$346 \quad (20) \quad \delta_{k+1} = \|w_k - P(t, \hat{w}_k)\|_2 \leq \|w_k - \hat{w}_k\|_2 \leq \left[(1 + Bh)\delta_k + F(h^2 + h\varepsilon) \right].$$

347 This is the same control as equation (13): the proof can be concluded in the same
348 way as above. \square

349 5. Numerical experiments.

350 **5.1. Setup.** We implemented the numerical scheme on simple manifolds where
351 the parallel transport is known in closed form, allowing us to evaluate the numerical
352 error ¹. We present two examples:

- 353 • \mathbb{S}^2 : in spherical coordinates (θ, ϕ) the metric is $g = \begin{pmatrix} 1 & 0 \\ 0 & \sin(\theta)^2 \end{pmatrix}$. We gave
354 expressions for geodesics and parallel transport in Section 2.3.
- 355 • The set of 3×3 symmetric positive-definite matrices SPD(3). The tangent
356 space at any points of this manifold is the set of symmetric matrices. In
357 [3], the authors endow this space with the affine-invariant metric: for $\Sigma \in$
358 SPD(3), $V, W \in \text{Sym}(3)$, $g_\Sigma(V, W) = \text{tr}(\Sigma^{-1}V\Sigma^{-1}W)$. Through an explicit
359 computation of the Christoffel symbols, they derive explicit expressions for
360 any geodesic $\Sigma(t)$ starting at $\Sigma_0 \in \text{SPD}(3)$ with initial tangent vector $X \in$
361 $\text{Sym}(3)$: $\Sigma(t) = \Sigma_0^{\frac{1}{2}} \exp(tX)\Sigma_0^{\frac{1}{2}}$ where $\exp : \text{Sym}(3) \rightarrow \text{SPD}(3)$ is the matrix
362 exponentiation. Deriving an expression for the parallel transport can also be
363 done using the explicit Christoffel symbols, see [11]. If $\Sigma_0 \in \text{SPD}(3)$ and
364 $X, W \in \text{Sym}(3)$, then

$$365 \quad P_{0,t}(W) = \exp\left(\frac{t}{2}X\Sigma_0^{-1}\right)W \exp\left(\frac{t}{2}\Sigma_0^{-1}X\right).$$

366 The code for this numerical scheme can be written in a generic way and used for
367 any manifold by specifying the Hamiltonian equations and the inverse of the metric.
368 For experiments in large dimensions, we refer to [7].

¹A modular Python version of the code is available here: <https://gitlab.icm-institute.org/maxime.louis/parallel-transport>

369 *Remark.* Note that even though the computation of the gradient of the inverse of
 370 the metric with respect to the position, $\nabla_x K$, is required to integrate the Hamiltonian
 371 equations (5), $\nabla_x K$ can be computed from the gradient of the metric using the fact
 372 that any smooth map $M : \mathbb{R} \rightarrow GL_n(\mathbb{R})$ verifies $\frac{dM^{-1}}{dt} = -M^{-1} \frac{dM}{dt} M^{-1}$. This is how
 373 we proceeded for SPD(3): it spares some potential difficulties if one does not have
 374 access to analytical expressions for the inverse of the metric. It is however a costly
 375 operation which requires the computation of the full inverse of the metric at each
 376 step.

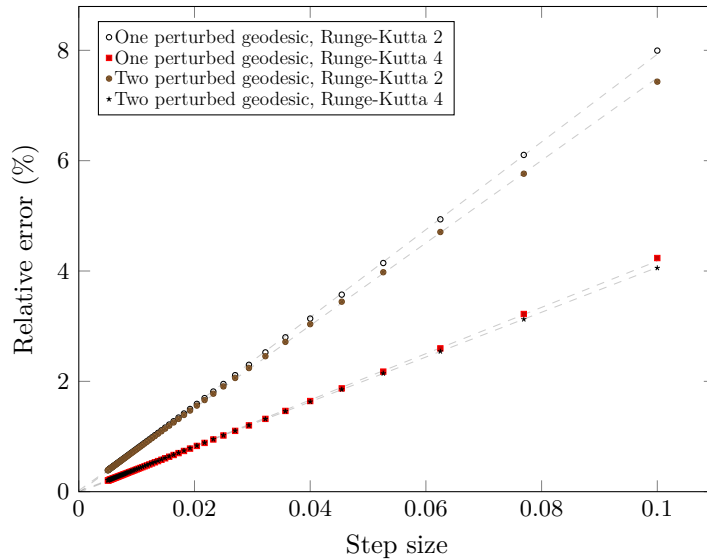


FIGURE 3. Relative error for the 2-Sphere in different settings, as functions of the step size, with initial point, velocity and initial w kept constant. The dotted lines are linear regressions of the measurements.

377 **5.2. Results.** Errors measured in the chosen system of coordinates confirm the
 378 linear behavior in both cases, as shown on Figures 3 and 4.

379 We assessed the effect of a higher order for the Runge-Kutta scheme in the in-
 380 tegration of geodesics. Using a fourth order method increases the accuracy of the
 381 transport in both cases, by a factor 2.3 in the single geodesic case. A fourth order
 382 method is twice as expensive as a second order method in terms of number of calls to
 383 the Hamiltonian equations, hence in this case it is the most efficient way to reach a
 384 given accuracy.

385 We also investigated the effect of using step (v). Doing so yields an exact transport
 386 for the sphere, because it is of dimension 2 and the conservation of two quantities is
 387 enough to ensure an exact transport, up to the fact that the geodesic is computed
 388 approximately, so that the actual observed error is the error in the integration of the
 389 geodesic equation. It yields a dramatically improved transport of the same order of
 390 convergence for SPD(3) (see Figure 4). The complexity of this operation is very low,
 391 and we recommend to always use it. It can be expected however that the effect of the
 392 enforcement of these conservations will lower as the dimension increases, since it only
 393 fixes two components of the transported vector.

394 We also confirmed numerically that without a second-order method to integrate

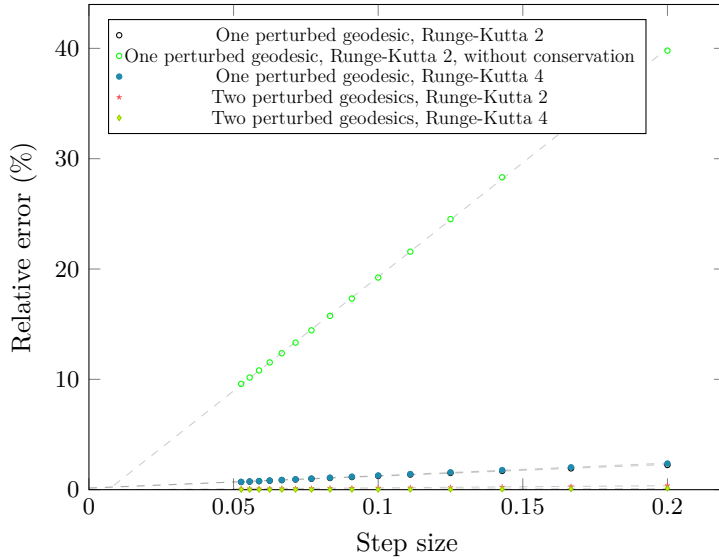


FIGURE 4. Relative errors for $SPD(3)$ in different settings, as functions of the step size, with initial point, velocity and initial w kept constant. The dotted lines are linear regressions. Runge-Kutta 2 (resp. 4) indicate that a second-order (resp. fourth order) Runge-Kutta integration has been used to integrate the geodesic equations at steps (i) and (ii). Without conservation indicates that (v) has not been used.

395 the geodesic equations at steps (i) and (ii) of the algorithm, the scheme does not con-
 396 verge. This is not in contradiction with Theorem 3.1 which supposes this integration
 397 is done with a second-order Runge Kutta.

398 Finally, using two geodesics to compute a central-finite difference for the Jacobi
 399 field is 1.5 times more expensive than using a single geodesic, in terms of number of
 400 calls to the Hamiltonian equations, and it is therefore more efficient to compute two
 401 perturbed geodesics in the case of the symmetric positive-definite matrices.

402 **5.3. Comparison with Schild’s ladder.** We compared the relative errors of
 403 the fanning scheme with Schild’s ladder. We implemented Schild’s ladder on the
 404 sphere and compared the relative errors of both schemes on a same geodesic and
 405 vector. We chose this vector to be orthogonal to the velocity, since the transport with
 406 Schild’s ladder is exact if the transported vector is colinear to the velocity. We use
 407 a closed form expression for the Riemannian logarithm in Schild’s ladder, and closed
 408 form expressions for the geodesic. The results are given in Figure 5.

409 **6. Conclusion.** We proposed a new method, the fanning scheme, to compute
 410 parallel transport along a geodesic on a Riemannian manifold using Jacobi fields. In
 411 contrast to Schild’s ladder, this method does not require the computation of Rie-
 412 mannian logarithms, which may not be given in closed form and potentially hard to
 413 approximate. We proved that the error of the scheme is of order $O(\frac{1}{N})$ where N
 414 is the number of discretization steps, and that it cannot be improved in the general
 415 case, yielding the same convergence rate as Schild’s ladder. We also showed that only
 416 four calls to the Hamiltonian equations are necessary at each step to provide a satis-
 417 fying approximation of the transport, two of them being used to compute the main
 418 geodesic.

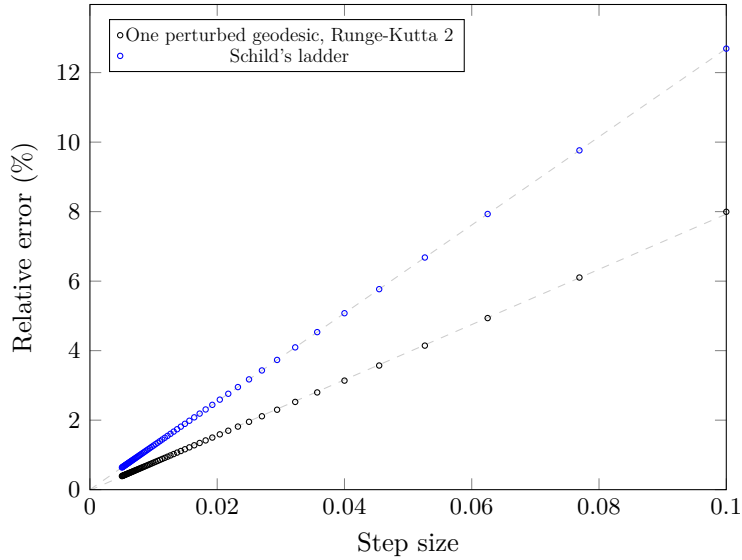


FIGURE 5. Relative error of Schild's ladder scheme compared to the fanning scheme (double geodesic, Runge-Kutta 2) proposed here, in the case of \mathbb{S}^2 .

419 A limitation of this scheme is to only be applicable when parallel transporting
 420 along geodesics, and this limitation seems to be unavoidable with the identity it relies
 421 on. Note also that the Hamiltonian equations are expressed in the cotangent space
 422 whereas the approximation of the transport computed at each step lies in the tangent
 423 space to the manifold. Going back and forth from cotangent to tangent space at
 424 each iteration is costly if the metric is not available in closed-form, as it requires the
 425 inversion of a system. In very high dimensions this might limit the performances

426 **Acknowledgements.** This work has been partially funded by the European Re-
 427 search Council (ERC) under grant agreement No 678304, European Union's Horizon
 428 2020 research and innovation programme under grant agreement No 666992, and the
 429 program "Investissements d'avenir" ANR-10-IAIHU-06.

430 **Appendix A. Pseudo-code for the algorithm.** We give a pseudo-code
 431 description of the numerical scheme. Here, $G(p)$ denotes the metric matrix at p for
 432 any $p \in \mathcal{M}$.

```

433 1: function PARALLELTRANSPORT( $x_0, \alpha_0, w_0, N$ )
434 2:   function  $V(x, \alpha)$ 
435 3:     return  $K(x)\alpha$ 
436 4:   end function
437
438 5:   function  $F(x, \alpha)$ 
439 6:     return  $-\frac{1}{2}\nabla_x (\alpha^T K(x)\alpha)$       ▷ in closed form or by finite differences
440 7:   end function

```

441
 442 ▷ γ_0 coordinates of $\gamma(0)$
 443 ▷ α_0 coordinates of $G(\gamma(0))\dot{\gamma}(0) \in T_{\gamma(0)}^*\mathcal{M}$
 444 ▷ w_0 coordinates of $w \in T_{\gamma(0)}\mathcal{M}$
 445 ▷ β_0 coordinates of $G(\gamma(0))w_0$

446 ▷ N number of time-steps

447 8: $h = 1/N, \varepsilon = 1/N$

448 9: **for** $k = 0, \dots, (N - 1)$ **do**

449 ▷ integration of the main geodesic

450 10: $\gamma_{k+\frac{1}{2}} = \gamma_k + \frac{h}{2}v_k$

451 11: $\alpha_{k+\frac{1}{2}} = \alpha_k + \frac{h}{2}F(\gamma_k, \alpha_k)$

452 12: $\gamma_{k+1} = \gamma_k + hV(\gamma_{k+\frac{1}{2}}, \alpha_{k+\frac{1}{2}})$

453 13: $\alpha_{k+1} = \alpha_k + hF(\gamma_{k+\frac{1}{2}}, \alpha_{k+\frac{1}{2}})$

454 ▷ perturbed geodesic equation in the direction w_k

455 14: $\gamma_{k+\frac{1}{2}}^\varepsilon = \gamma_k + \frac{h}{2}v(\gamma_k, \alpha_k + \varepsilon\beta_k)$

456 15: $\alpha_{k+\frac{1}{2}}^\varepsilon = \alpha_k + \varepsilon\beta_k + \frac{h}{2}F(\gamma_k^\varepsilon, \alpha_k + \varepsilon\beta_k)$

457 16: $\gamma_{k+1}^\varepsilon = \gamma_k^\varepsilon + hV(\gamma_{k+\frac{1}{2}}^\varepsilon, \alpha_{k+\frac{1}{2}}^\varepsilon)$

458 ▷ Jacobi field by finite differences

459 17: $\hat{w}_{k+1} = \frac{\gamma_{k+1}^\varepsilon - \gamma_{k+1}}{h\varepsilon}$

460 18: $\hat{\beta}_{k+1} = g(\gamma_{k+1})w_{k+1}$ ▷ Use explicit g or solve $K(\gamma_{k+1})\hat{\beta}_{k+1} = \hat{w}_{k+1}$

461 ▷ Conserve quantities

462 19: Solve for a, b :

464 20: $\beta_0^\top K(\gamma_0)\beta_0 = (a\hat{\beta}_{k+1} + b\alpha_{k+1})^\top K(\tilde{\gamma}_{k+1})(a\hat{\beta}_{k+1} + b\alpha_{k+1}),$

465 21: $\alpha_0^\top K(\gamma_0)\alpha_0 = (a\hat{\beta}_{k+1} + b\alpha_{k+1})^\top K(\tilde{\gamma}_{k+1})(a\hat{\beta}_{k+1} + b\alpha_{k+1}, v_{k+1})$

467 22: $\beta_{k+1} = a\hat{\beta}_{k+1} + b\alpha_{k+1}$ ▷ parallel transport

468 23: $w_{k+1} = K(\gamma_{k+1})\beta_{k+1}$

469 24: **end for**

470 **return** γ_N, α_N, w_N

471 ▷ γ_N approximation of $\gamma(1)$

472 ▷ α_N approximation of $G(\gamma(1))\dot{\gamma}(1)$

473 ▷ w_N approximation of $P_{\gamma(0), \gamma(1)}(w_0)$

474 25: **end function**

475

476 Appendix B. Proofs.

477 **B.1. A lemma to change coordinates.** We recall that we suppose the geode-
 478 sic contained within a compact subset Ω of the manifold \mathcal{M} . We start with a result
 479 controlling the norms of change-of-coordinates matrices. Let p in \mathcal{M} and $q = \text{Exp}_p(v)$
 480 where $\|v\|_g \leq \frac{\eta}{2}$, where $\eta > 0$ is a lower bound on the injectivity radius on Ω . We
 481 consider two basis of $T_q\mathcal{M}$: one defined from the global system of coordinates, that
 482 we denote B_q^Φ , and another made of the normal coordinates centered at p , built from
 483 the coordinate on $T_p\mathcal{M}$ obtained from the coordinate chart Φ , that we denote B_q^N .
 484 We can therefore define $\Lambda(p, q)$ as the change-of-coordinates matrix between B_q^Φ and
 485 B_q^N . The operator norms $\|\cdot\|$ of these matrices are bounded over Ω in the following
 486 sense:

487 LEMMA B.1. *There exists $L \geq 0$ such that for all $p \in K$ and for all $q \in K$ such*
 488 *that $q = \text{Exp}_p(v)$ for some $v \in T_p\mathcal{M}$ with $\|v\|_g \leq \frac{\eta}{2}$, we have*

$$489 \quad \|\Lambda(p, q)\| \leq L$$

490 and

$$491 \quad \|\Lambda^{-1}(p, q)\| \leq L.$$

492 *Proof.* Any two norms on $T_q\mathcal{M}$ are equivalent, and the norm bounds of the coordi-
 493 nate change smoothly depend on p and q by smoothness of the metric. Hence the
 494 result. \square

495 This lemma allows us to translate any bound on the components of a tensor in the
 496 global system of coordinates into a bound on the components of the same tensor in
 497 any of the normal systems of coordinates centered at a point of the geodesic, and *vice*
 498 *versa*.

499 **B.2. Transport and connection.** We prove a result connecting successive co-
 500 variant derivatives to parallel transport:

501 PROPOSITION B.2. *Let V be a vector field on \mathcal{M} . Let $\gamma : [0, 1] \rightarrow \mathcal{M}$ be a geodesic.*
 502 *Then*

$$503 \quad (21) \quad \nabla_{\dot{\gamma}}^k V(\gamma(t)) = \left. \frac{d^k}{dh^k} \right|_{h=0} P_{t,t+h}^{-1}(V(\gamma(t+h))).$$

504 *Proof.* Let $E_i(0)$ be an orthonormal basis of $T_{\gamma(0)}\mathcal{M}$. Using the parallel transport
 505 along γ , we get orthonormal basis $E_i(s)$ of $T_{\gamma(t)}\mathcal{M}$ for all t . For $t \in [0, 1]$, denote
 506 $(a_i(t))_{i=1,\dots,n}$ the coordinates of $V(\gamma(t))$ in the basis $(E_i(t))_{i=1,\dots,n}$. We have

$$507 \quad \frac{d^k}{dh^k} P_{t,t+h}^{-1}(V(\gamma(t+h))) = \frac{d^k}{dh^k} P_{t,t+h}^{-1} \left(\sum_{i=1}^n a_i(t+h) E_i(t+h) \right) = \sum_{i=1}^n \frac{d^k a_i(t+h)}{dh^k} E_i(t)$$

508 because $P_{t,t+h}^{-1} E_i(t+h) = E_i(t)$ does not depend on h . On the other hand

$$509 \quad \nabla_{\dot{\gamma}}^k V(\gamma(t)) = \nabla_{\dot{\gamma}}^k \sum_{i=1}^n a_i(t) E_i(t) = \sum_{i=1}^n \nabla_{\dot{\gamma}}^k (a_i(t)) E_i(t) = \sum_{i=1}^n \frac{d^k a_i(t+h)}{dh^k} E_i(t)$$

510 by definition of $E_i(s)$. \square

511 **B.3. A stronger version of Proposition 2.1.** From there, we can prove a
 512 stronger version of Proposition 2.1. As before, η denotes a lower bound on the injec-
 513 tivity radius of \mathcal{M} on Ω .

514 PROPOSITION B.3. *There exists $A \geq 0$ such that for all $t \in [0, 1[$, for all $w \in$
 515 $T_{\gamma(t)}\mathcal{M}$ and for all $h < \frac{\eta}{\|\dot{\gamma}(t)\|_g}$ we have*

$$516 \quad \left\| P_{t,t+h}(w) - \frac{J_{\gamma(t)}^w(h)}{h} \right\|_g \leq Ah^2 \|w\|_g.$$

517 *Proof.* Let $t \in [0, 1[$, $w \in T_{\gamma(t)}\mathcal{M}$ and $h < \frac{\eta}{\|\dot{\gamma}(t)\|_g}$ i.e. such that $J_{\gamma(t)}^w(h)$ is well
 518 defined. From Lemma B.2, for any smooth vector field V on \mathcal{M} ,

$$519 \quad (22) \quad \nabla_{\dot{\gamma}(t)}^k V(\gamma(t)) = \left. \frac{d^k}{dh^k} \right|_{h=0} P_{t,t+h}^{-1}(V(\gamma(t+h))).$$

520 We will use this identity to obtain a development of $V(\gamma(t+h)) = J_{\gamma(t)}^w(h)$ for small
 521 h .

522 We have $J_{\gamma(t)}^w(0) = 0$, $\nabla_{\dot{\gamma}} J_{\gamma(t)}^w(0) = w$, $\nabla_{\dot{\gamma}}^2 J_{\gamma(t)}^w(0) = -R(J_{\gamma(t)}^w(0), \dot{\gamma}(0))\dot{\gamma}(0) = 0$
 523 using equation (1) and finally

$$524 \quad (23) \quad \begin{aligned} \|\nabla_{\dot{\gamma}}^3 J_{\gamma(t)}^w(h)\|_g &= \|\nabla_{\dot{\gamma}}(R)(J_{\gamma(t)}^w(h), \dot{\gamma}(h))\dot{\gamma}(h) + R(\nabla_{\dot{\gamma}} J_{\gamma(t)}^w(h), \dot{\gamma}(h))\dot{\gamma}(h)\|_g \\ &\leq \|\nabla_{\dot{\gamma}} R\|_{\infty} \|\dot{\gamma}(h)\|_g^2 \|J_{\gamma(t)}^w(h)\|_g + \|R\|_{\infty} \|\dot{\gamma}(h)\|_g^2 \|\nabla_{\dot{\gamma}} J_{\gamma(t)}^w(h)\|_g, \end{aligned}$$

525 where the ∞ -norms, taken over the geodesic and the compact Ω , are finite because the
 526 curvature and its derivatives are bounded. **Note that we used $\nabla_{\dot{\gamma}}\dot{\gamma} = 0$ which holds**
 527 **since γ is a geodesic.** In normal coordinates centered at $\gamma(t)$, we have $J_{\gamma(t)}^w(h)^i =$
 528 hw^i . Therefore, if we denote $g_{ij}(\gamma(t+h))$ the components of the metric in normal
 529 coordinates, we get using Einstein notations

$$530 \quad \|J_{\gamma(t)}^w(h)\|_g^2 = h^2 g_{ij}(\gamma(t+h)) w^i w^j.$$

531 To obtain an upper bound for this term which does not depend on t , we note that the
 532 coefficients of the metric in the global coordinate system are bounded on Ω . Using
 533 Lemma B.1, we get a bound $M \geq 0$ valid on all the systems of normal coordinates
 534 centered at a point of the geodesic, so that

$$535 \quad \|J_{\gamma(t)}^w(h)\|_g \leq hM\|w\|_2.$$

536 By equivalence of the norms as seen in Lemma (B.1), and because g varies smoothly,
 537 there exists $N \geq 0$ such that

$$538 \quad (24) \quad \|J_{\gamma(t)}^w(gh)\|_g \leq hMN\|w\|_g$$

539 where the dependence of the majoration on t has vanished, and the result stays valid
 540 for all $h < \max(\frac{\eta}{\|\dot{\gamma}(t)\|_g}, 1-t)$ and all w . Similarly, there exists $C > 0$ such that

$$541 \quad (25) \quad \|\nabla_{\dot{\gamma}} J_{\gamma(s)}^w(h)\| \leq C\|w\|_g,$$

542 at any point and for any $h < \max(\frac{\eta}{\|\dot{\gamma}(t)\|_g}, 1-t)$. Gathering equations (23), (24) and
 543 (25), we get that there exists a constant $A \geq 0$ which does not depend on t , h or w
 544 such that

$$545 \quad (26) \quad \left\| \nabla_{\dot{\gamma}}^3 J_{\gamma(s)}^w(h) \right\|_g \leq A\|w\|_g.$$

546 Now using equation (22) with $V(\gamma(t+h)) = J_{\gamma(t)}^w(h)$ and a Taylor's formula, we get

$$547 \quad P_{t,t+h}^{-1}(J_{\gamma(t)}^w(h)) = hw + h^3 r(h, w)$$

548 where r is the remainder of the expansion, controlled in equation (26). We thus get

$$549 \quad \left\| \frac{J_{\gamma(t)}^w(h)}{h} - P_{t,t+h}(w) \right\|_g = \|P_{t,t+h}(h^3 r(w, h))\|_g.$$

550 Now, because the parallel transport is an isometry, we can use our control (26) on the
 551 remainder to get

$$552 \quad \left\| \frac{J_{\gamma(t)}^w(h)}{h} - P_{t,t+h}(w) \right\|_g \leq \frac{A}{6} h^2 \|w\|_g. \quad \square$$

553 **B.4. A Lemma to control error accumulation.** At every step of the scheme,
 554 we compute a Jacobi field from an approximate value of the transported vector. We
 555 need to control the error made with this computation from an already approximate
 556 vector. We provide a control on the 2-norm of the corresponding error, in the global
 557 system of coordinates.

558 LEMMA B.4. *There exists $B \geq 0$ such that for all $t \in [0, 1[$, for all $w_1, w_2 \in$
559 $T_{\gamma(t)}\mathcal{M}$ and for all $h \leq \frac{\eta}{\|\dot{\gamma}(t)\|_g}$ small enough, we have :*

$$560 \quad (27) \quad \left\| \frac{J_{\gamma(t)}^{w_1}(h) - J_{\gamma(t)}^{w_2}(h)}{h} \right\|_2 \leq (1 + Bh)\|w_1 - w_2\|_2.$$

561 *Proof.* Let $t \in [0, 1[$ and $h \leq \frac{\eta}{\|\dot{\gamma}(t)\|_g}$. We denote $p = \gamma(t)$, $q = \gamma(t+h)$. We use the
562 exponential map to get normal coordinates on a neighborhood V of p from the basis
563 $(\frac{\partial}{\partial x^i}|_p)_{i=1, \dots, n}$ of $T_p\mathcal{M}$. Let's denote $(\frac{\partial}{\partial y^i}|_r)_{i=1, \dots, n}$ the basis obtained in the tangent
564 space at any point r of V from this system of normal coordinates centered at p . At any
565 point r in V , there are now two different bases of $T_r\mathcal{M}$: $(\frac{\partial}{\partial y^i}|_r)_{i=1, \dots, n}$ obtained from
566 the normal coordinates and $(\frac{\partial}{\partial x^i}|_r)_{i=1, \dots, n}$ obtained from the coordinate system Φ .
567 Let $w_1, w_2 \in T_p\mathcal{M}$ and denote w_j^i for $i \in \{1, \dots, n\}$, $j \in \{1, 2\}$ the coordinates in the
568 global system Φ . By definition, the basis $(\frac{\partial}{\partial y^i}|_p)_{i=1, \dots, n}$ and the basis $(\frac{\partial}{\partial x^i}|_p)_{i=1, \dots, n}$
569 coincide, and in particular, for $j \in \{1, 2\}$:

$$570 \quad w_j = (w_j^i) \frac{\partial}{\partial x^i} \Big|_p = (w_j^i) \frac{\partial}{\partial y^i} \Big|_p.$$

571 If $i \in \{1, \dots, n\}$, $j \in \{1, 2\}$, the j -th coordinate of $J_{\gamma(t)}^{w_j^i}(h)$ in the basis $(\frac{\partial}{\partial y^i}|_q)_{i=1, \dots, n}$
572 is

$$573 \quad J_{\gamma(t)}^{w_j^i}(h)^i = \frac{\partial}{\partial \varepsilon} \Big|_{\varepsilon=0} (\text{Exp}_p(h(v + \varepsilon w_j)))^i = \frac{\partial}{\partial \varepsilon} \Big|_{\varepsilon=0} (h(v + \varepsilon w_j))^i = h w_j^i.$$

574 Let $\Lambda(\gamma(t+h), \gamma(t))$ be the change-of-coordinate matrix of $T_{\gamma(t+h)}$ from the basis
575 $(\frac{\partial}{\partial y^i}|_q)_{i=1, \dots, n}$ to the basis $(\frac{\partial}{\partial x^i}|_q)_{i=1, \dots, n}$. Λ varies smoothly with t and h , and is
576 the identity when $h = 0$. Hence, we can write an expansion

$$577 \quad \Lambda(\gamma(t+h), \gamma(t)) = Id + hW(t) + O(h^2).$$

578 The second order term depends on the second derivative of Λ with respect to h .
579 Restricting ourselves to a compact subset of \mathcal{M} , as in Lemma B.1, we get a uniform
580 bound on the norm of this second derivative thus getting a control on the operator
581 norm of $\Lambda(\gamma(t+h), \gamma(t))$, that we can write, for h small enough

$$582 \quad \|\Lambda(\gamma(t+h), \gamma(t))\| \leq (1 + Bh)$$

583 where B is a positive constant which does not depend on h or t . Now we get

$$584 \quad \left\| \frac{J_{\gamma(t)}^{w_1}(h) - J_{\gamma(t)}^{w_2}(h)}{h} \right\|_2 = \|\Lambda(\gamma(t+h), \gamma(t))(w_1 - w_2)\|_2 \leq (1 + Bh)\|w_1 - w_2\|_2$$

585 which is the desired result. \square

586 **B.5. Proof that we can compute the geodesic simultaneously with a**
587 **second-order method.** We give here a control on the error made in the scheme

588 when computing the main geodesic approximately and simultaneously with the par-
 589 allel transport. We assume that the main geodesic is computed with a second-order
 590 method, and we need to control the subsequent error on the Jacobi field. The com-
 591 putations are made in global coordinates, and the error measured by the 2-norm in
 592 these coordinates. $\Phi : \Omega \rightarrow U$ denotes the corresponding diffeomorphism. We note
 593 $\eta > 0$ a lower bound on the injectivity radius of \mathcal{M} on Ω and $\varepsilon > 0$ the parameter
 594 used to compute the perturbed geodesics at step (ii).

595 **PROPOSITION B.5.** *There exists $A > 0$ such that for all $t \in [0, 1[$, for all $h \in$
 596 $[0, 1 - t]$, for all $w \in T_{\gamma(t)}\mathcal{M}$:*

$$597 \quad \left\| \frac{J_{\gamma_k}^{\tilde{w}_k}(h)}{h} - \frac{J_{\tilde{\gamma}_k}^{\tilde{w}_k}(h)}{h} \right\|_2 \leq Ah^2.$$

598 *Proof.* Let $t \in [0, 1[$, $h \in [0, 1 - t]$, and $w \in T_{\gamma(t)}\mathcal{M}$. The term rewrites

$$(28) \quad \left\| \frac{J_{\gamma_k}^{\tilde{w}_k}(h)}{h} - \frac{J_{\tilde{\gamma}_k}^{\tilde{w}_k}(h)}{h} \right\|_2 = \left\| \frac{\partial \text{Exp}_{\gamma_k}(h\dot{\gamma}_k + x\tilde{w}_k)}{\partial x} \Big|_{x=0} - \frac{\partial \text{Exp}_{\tilde{\gamma}_k}(h\tilde{\dot{\gamma}}_k + x\tilde{w}_k)}{\partial x} \Big|_{x=0} \right\|_2.$$

600 This is the difference between the derivatives of two solutions of the same differential
 601 equation (5) with two different initial conditions. More precisely, we define $\Pi : \Phi(\Omega) \times$
 602 $B_{\mathbb{R}^n}(0, \|\tilde{\gamma}_k\| + 2\varepsilon\|\tilde{w}_k\|) \times [0, \eta] \rightarrow \mathbb{R}^n$ such that $\Pi(p_0, \alpha_0, h)$ are the coordinates of the
 603 solutions of the Hamiltonian equation at time h with initial coordinates p_0 and initial
 604 momentum α_0 . Π is the flow, in coordinates, of the geodesic equation. We can now
 605 rewrite equation (28)

$$606 \quad \left\| \frac{J_{\gamma_k}^{\tilde{w}_k}(h)}{h} - \frac{J_{\tilde{\gamma}_k}^{\tilde{w}_k}(h)}{h} \right\|_2 = \left\| \frac{\partial \Pi(\gamma_k, \dot{\gamma}_k + \varepsilon\tilde{w}_k, h)}{\partial \varepsilon} \Big|_{\varepsilon=0} - \frac{\partial \Pi(\tilde{\gamma}_k, \tilde{\dot{\gamma}}_k + \varepsilon\tilde{w}_k, h)}{\partial \varepsilon} \Big|_{\varepsilon=0} \right\|_2.$$

607 By Cauchy-Lipschitz theorem and results on the regularity of the flow, Π is smooth.
 608 Hence, its derivatives are bounded over its compact set of definition. Hence there
 609 exists a constant $A > 0$ such that

$$610 \quad \left\| \frac{J_{\gamma_k}^{\tilde{w}_k}(h)}{h} - \frac{J_{\tilde{\gamma}_k}^{\tilde{w}_k}(h)}{h} \right\|_2 \leq A (\|\tilde{\gamma} - \gamma\|_2 + \|\dot{\tilde{\gamma}} - \dot{\gamma}\|_2)$$

611 where we can once again assume A independent of t and h . In coordinates, we use a
 612 second-order Runge-Kutta method to integrate the geodesic equation (5) so that the
 613 cumulated error $\|\tilde{\gamma} - \gamma\|_2 + \|\dot{\tilde{\gamma}} - \dot{\gamma}\|_2$ is of order h^2 . Hence, there exists a positive
 614 constant B which does not depend on h , t or w such that

$$615 \quad \left\| \frac{J_{\gamma_k}^{\tilde{w}_k}(h)}{h} - \frac{J_{\tilde{\gamma}_k}^{\tilde{w}_k}(h)}{h} \right\|_2 \leq Bh^2. \quad \square$$

616 **B.6. Numerical approximation with a single perturbed geodesic.** We
 617 prove a lemma which allows to control the error we make when we approximate
 618 numerically the Jacobi field using steps (iii) and (ii) of the algorithm:

619 **LEMMA B.6.** *For all $L > 0$, there exists $A > 0$ such that for all $t \in [0, 1[$, for
 620 all $h \in [0, \frac{\eta}{\|\tilde{\gamma}(t)\|_\sigma}]$ and for all $w \in T_{\gamma(t)}\mathcal{M}$ with $\|w\|_2 < L$ - in the global system of*

621 *coordinates – we have*

$$622 \quad \left\| \frac{J_{\gamma(t)}^w(h) - \tilde{J}_{\gamma(t)}^w(h)}{h} \right\|_2 \leq A(h^2 + \varepsilon h)$$

623 *where $\tilde{J}_{\gamma(t)}^w(h)$ is the numerical approximation of $J_{\gamma(t)}^w(h)$ computed with a single per-*
 624 *turbed geodesic and a first-order differentiation method.*

625 *Proof.* Let $L > 0$. Let $t \in [0, 1[$, $h \in [0, \frac{\eta}{\|\dot{\gamma}(t)\|_g}]$ and $w \in T_{\gamma(t)}\mathcal{M}$. We split the
 626 error term into two parts

$$627 \quad \left\| \frac{J_{\gamma(t)}^w(h)}{h} - \frac{\tilde{J}_{\gamma(t)}^w(h)}{h} \right\|_2 \leq \underbrace{\left\| \frac{J_{\gamma(t)}^w(h)}{h} - \frac{\text{Exp}_{\gamma(t)}(h\dot{\gamma}(t) + \varepsilon w) - \text{Exp}_{\gamma(t)}(h\dot{\gamma}(t))}{\varepsilon h} \right\|_2}_{(1)} +$$

$$\underbrace{\left\| \frac{\text{Exp}_{\gamma(t)}(h\dot{\gamma}(t) + \varepsilon w) - \text{Exp}_{\gamma(t)}(h\dot{\gamma}(t)) - \tilde{\text{Exp}}_{\gamma(t)}(h\dot{\gamma}(t) + \varepsilon w) + \tilde{\text{Exp}}_{\gamma(t)}(h\dot{\gamma}(t))}{\varepsilon h} \right\|_2}_{(2)}$$

628 where Exp is the Riemannian exponential and $\tilde{\text{Exp}}$ is the numerical approximation of
 629 this Riemannian exponential computed thanks to the Hamiltonian equations. When
 630 running the scheme, these computations are done in the global system of coordinates.

631 *Term (1).* Let $i \in \{1, \dots, n\}$ and let $F^i : (x, t, w) \mapsto \text{Exp}[h\dot{\gamma}(t) + xw]^i$. We have

$$632 \quad \begin{aligned} & \frac{J_{\gamma(t)}^w(h)^i}{h} - \frac{\text{Exp}[h\dot{\gamma}(t) + \varepsilon w]^i - \text{Exp}[h\dot{\gamma}(t)]^i}{\varepsilon h} \\ &= \frac{1}{h} \frac{\partial F^i(\varepsilon h, t, w)}{\partial \varepsilon} \Big|_{\varepsilon=0} - \frac{F^i(\varepsilon h, t, w) - F^i(0, t, w)}{\varepsilon h} \\ &= \frac{\partial F^i(x, t, w)}{\partial x} \Big|_{x=0} - \frac{F^i(\varepsilon h, t, w) - F^i(0, t, w)}{\varepsilon h}. \end{aligned}$$

This is the error when performing a first-order differentiation on $x \mapsto F^i(x, t, w)$ at 0. This error is of order εh and will depend smoothly on t and w . Since $t \in [0, 1]$ and imposing $\|w\|_2 < L$, there exists B which does not depend on t or w such that

$$\left| \frac{J_{\gamma(t)}^w(h)^i}{h} - \frac{\text{Exp}[h\dot{\gamma}(t) + \varepsilon h w]^i - \text{Exp}[h\dot{\gamma}(t)]^i}{\varepsilon h} \right| \leq B\varepsilon h$$

so that there exists $C > 0$ such that for all t , for all h and for all w with $\|w\|_2 \leq L$

$$\left\| \frac{J_{\gamma(t)}^w(h)}{h} - \frac{\text{Exp}[h\dot{\gamma}(t) + \varepsilon h w] - \text{Exp}[h\dot{\gamma}(t)]}{\varepsilon h} \right\|_2 \leq C\varepsilon h.$$

633

634 *Term (2).* We rewrite the Hamiltonian equation $\dot{x}(t) = F_1(x(t), \alpha(t))$ and $\dot{\alpha}(t) =$
 635 $F_2(x(t), \alpha(t))$. We denote $x^\varepsilon, \alpha^\varepsilon$ the solution of this equation (in the global sys-
 636 tem of coordinates) with initial conditions $x^\varepsilon(0) = x_0 = \gamma(t)$ and $\alpha^\varepsilon(0) = \alpha_0^\varepsilon =$
 637 $K(x_0)^{-1}(\dot{\gamma}(t) + \varepsilon w)$. We denote \tilde{x}^ε the result after one step of length h of the integra-
 638 tion of the same equation using a second-order Runge-Kutta method with parameter

639 $\delta \in]0, 1]$. The term (2) rewrites

$$640 \quad \frac{1}{\varepsilon h} \|(x^\varepsilon(h) - x^0(h)) - (\tilde{x}^\varepsilon - \tilde{x}^0)\|_2.$$

641 First, we develop x^ε in the neighborhood of 0:

$$642 \quad (29) \quad x^\varepsilon(h) = x_0 + h\dot{x}_0 + \frac{h^2}{2}\ddot{x}_0 + \int_0^h \frac{(h-t)^2}{2} \ddot{x}^\varepsilon(t) dt.$$

643 We have, for the last term:

$$644 \quad \left\| \int_0^h \frac{(h-t)^2}{2} \ddot{x}^\varepsilon(t) dt - \int_0^h \frac{(h-t)^2}{2} \ddot{x}^0(t) dt \right\|_2 = \left\| \int_0^h \int_0^{+\varepsilon} \frac{(h-t)^2}{2} \partial_\varepsilon \ddot{x}^\varepsilon(u, t) du dt \right\|_2,$$

645 x^ε being solution of a smooth ordinary differential equation with smoothly varying
646 initial conditions, it is smooth in time and with respect to ε . Hence, when the initial
647 conditions are within a compact, $\partial_\varepsilon \ddot{x}^\varepsilon$ is bounded, hence there exists $D > 0$ such that

$$648 \quad \left\| \int_0^h \frac{(h-t)^2}{2} \ddot{x}^\varepsilon(t) dt - \int_0^h \frac{(h-t)^2}{2} \ddot{x}^0(t) dt \right\|_2 \leq Dh^3\varepsilon.$$

649 After computations of the first and second order terms, we get:

$$650 \quad (30) \quad \begin{aligned} x^\varepsilon(h) = & x_0 + h(\dot{\gamma}(0) + \varepsilon w) + \\ & \frac{h^2}{2} \left((\nabla_x K)(x_0)[K(x_0)\alpha_0^\varepsilon]\alpha_0^\varepsilon + K(x_0)F_2(x_0, \alpha_0^\varepsilon) \right) + O(h^3|\varepsilon|) \end{aligned}$$

651 Now we focus on the approximation \tilde{x}^ε . One step of a second-order Runge Kutta with
652 parameter δ gives:

$$653 \quad \begin{aligned} \tilde{x}^\varepsilon &= x_0 + h \left[\left(1 - \frac{1}{2\delta}\right) F_1(x_0, \alpha_0^\varepsilon) + \frac{1}{2\delta} F_1(x_0 + \delta h F_1(x_0, \alpha_0^\varepsilon), \alpha_0^\varepsilon + \delta h F_2(x_0, \alpha_0^\varepsilon)) \right] \\ &= x_0 + h \left[\left(1 - \frac{1}{2\delta}\right) K(x_0)\alpha_0^\varepsilon + \frac{1}{2\delta} K(x_0 + \delta h K(x_0)\alpha_0^\varepsilon)(\alpha_0^\varepsilon + \delta h F_2(x_0, \alpha_0^\varepsilon)) \right] \end{aligned}$$

654 We use a Taylor expansion for K :

$$655 \quad \begin{aligned} K(x_0 + \delta h K(x_0)\alpha_0^\varepsilon) &= K(x_0) + \delta h (\nabla_x K)(x_0)[K(x_0)\alpha_0^\varepsilon] + \\ & \quad \frac{(\delta h)^2}{2} (\nabla_x K)^2[K(x_0)\alpha_0^\varepsilon, K(x_0)\alpha_0^\varepsilon] + O(h^3) \end{aligned}$$

656 Injecting this into the previous expression for x^ε , we get after development:

$$657 \quad \begin{aligned} \tilde{x}^\varepsilon &= x_0 + hK(x_0)(\alpha_0^\varepsilon) \\ &+ \frac{h^2}{2} [K(x_0)F_2(x_0, \alpha_0^\varepsilon) + (\nabla_x K)(x_0)[K(x_0)\alpha_0^\varepsilon]\alpha_0^\varepsilon] \\ &+ \frac{h^3\delta}{4} [(\nabla_x K)(x_0)[\alpha_0^\varepsilon]F_2(x_0, \alpha_0^\varepsilon) + (\nabla_x K)^2[K(x_0)\alpha_0^\varepsilon, K(x_0)\alpha_0^\varepsilon]\alpha_0^\varepsilon] + O(h^4) \end{aligned}$$

658 The third order terms of $\tilde{x}^\varepsilon - x^0$ is then proportionnal to:

$$659 \quad \begin{aligned} & (\nabla_x K)(x_0)[\alpha_0^\varepsilon]F_2(x_0, \alpha_0^\varepsilon) - (\nabla_x K)(x_0)\alpha_0^0 F_2(x_0, \alpha_0^0) \\ &+ (\nabla_x K)^2[K(x_0)\alpha_0^\varepsilon, K(x_0)\alpha_0^\varepsilon]\alpha_0^\varepsilon - (\nabla_x K)^2[K(x_0)\alpha_0^0, K(x_0)\alpha_0^0]\alpha_0^0 \end{aligned}$$

660 Both these terms are the differences of smooth functions at points whose distance is
 661 of order $\varepsilon\|w\|_2$. Because those functions are smooth, and we are only interested in
 662 these majorations for points in Ω and tangent vectors in a compact ball in the tangent
 663 space, this third order term is bounded by $Eh^3\varepsilon\|w\|_2$ where E is a positive constant
 664 which does not depend on the position on the geodesic. Finally, the zeroth, first and
 665 second-order terms of x^ε and \tilde{x}^ε cancel each other, so that there exists $D \geq 0$ such
 666 that:

$$667 \quad \|(x^\varepsilon(h) - x^0(h)) - (\tilde{x}^\varepsilon(h) - \tilde{x}^0(h))\|_2 \leq (h^3\varepsilon + Eh^3\varepsilon)$$

668 which concludes. \square

669 **B.7. Numerical approximation with two perturbed geodesics.** We sup-
 670 pose here that the computation to get the Jacobi field is done using two perturbed
 671 geodesics, and a second-order differentiation as described in equation (8).

672 LEMMA B.7. *For all $L > 0$, there exists $A > 0$ such that for all $t \in [0, 1[$, for
 673 all $h \in [0, 1 - t]$ and for all $w \in T_{\gamma(t)}\mathcal{M}$ with $\|w\|_2 < L$ -in the global system of
 674 coordinates - we have*

$$675 \quad \left\| \frac{J_{\gamma(t)}^w(h) - \tilde{J}_{\gamma(t)}^w(h)}{h} \right\|_2 \leq A(h^2 + \varepsilon h),$$

676 where $\tilde{J}_{\gamma(t)}^w(h)$ is the numerical approximation of $J_{\gamma(t)}^w(h)$ computed with two perturbed
 677 geodesics and a central finite differentiation method. We consider that this approxi-
 678 mation is computed in the global system of coordinates.

679 The proof is similar to the one above.

680

REFERENCES

- 681 [1] Arnol'd, V.I.: Mathematical methods of classical mechanics, vol. 60. Springer Science & Busi-
 682 ness Media (2013)
- 683 [2] Kheyfets, A., Miller, W.A., Newton, G.A.: Schild's ladder parallel transport procedure for
 684 an arbitrary connection. International Journal of Theoretical Physics **39**(12), 2891–2898
 685 (2000)
- 686 [3] Lenglet, C., Rousson, M., Deriche, R., Faugeras, O.: Statistics on the manifold of multivariate
 687 normal distributions: Theory and application to diffusion tensor mri processing. Journal
 688 of Mathematical Imaging and Vision **25**(3), 423–444 (2006)
- 689 [4] Lorenzi, M., Ayache, N., Pennec, X.: Schild's ladder for the parallel transport of deformations
 690 in time series of images. In: Biennial International Conference on Information Processing
 691 in Medical Imaging, pp. 463–474. Springer (2011)
- 692 [5] Lorenzi, M., Pennec, X.: Geodesics, parallel transport & one-parameter subgroups for dif-
 693 feomorphic image registration. International journal of computer vision **105**(2), 111–127
 694 (2013)
- 695 [6] Lorenzi, M., Pennec, X.: Parallel transport with pole ladder: application to deformations of
 696 time series of images. In: Geometric Science of Information, pp. 68–75. Springer (2013)
- 697 [7] Louis, M., Bône, A., Charlier, B., Durrleman, S., Initiative, A.D.N., et al.: Parallel transport
 698 in shape analysis: a scalable numerical scheme. In: International Conference on Geometric
 699 Science of Information, pp. 29–37. Springer (2017)
- 700 [8] Manfredo, P.: Riemannian geometry (1992)
- 701 [9] Rumpf, M., Wirth, B.: Variational time discretization of geodesic calculus. IMA Journal of
 702 Numerical Analysis **35**(3), 1011–1046 (2014)
- 703 [10] Schiratti, J.B., Allasonniere, S., Colliot, O., Durrleman, S.: Learning spatiotemporal trajec-
 704 tories from manifold-valued longitudinal data. In: Advances in Neural Information Processing
 705 Systems, pp. 2404–2412 (2015)

- 706 [11] Schiratti, J.B., Allasonniere, S., Colliot, O., Durrleman, S.: A Bayesian mixed-effects model to
707 learn trajectories of changes from repeated manifold-valued observations (2016). Accepted
708 at Journal of Machine Learning Research.
- 709 [12] Younes, L.: Jacobi fields in groups of diffeomorphisms and applications. Quarterly of applied
710 mathematics pp. 113–134 (2007)
- 711 [13] Younes, L.: Shapes and diffeomorphisms, vol. 171. Springer Science & Business Media (2010)
- 712 [14] Zhang, M., Fletcher, P.T.: Probabilistic principal geodesic analysis. In: Advances in Neural
713 Information Processing Systems, pp. 1178–1186 (2013)